Stem Cells Translational Medicine, 2026, **15**, szaf071
https://doi.org/10.1093/stcltm/szaf071
Original Research

Therapeutic effect of amniotic membrane mesenchymal stem cell-derived exosome-rich conditioned medium in cerebral palsy model

Eun-Jung Yoon[1,2,‡], Jiwon Jeong[1,‡], Yunseo Choi[1], Dae Hwan Kim[3], Tae Myoung Kim[4], Ehn-Kyoung Choi[5], Yun-Bae Kim[5,*], Dongsun Park[1,*]

[1]Laboratory of Veterinary Toxicology, College of Veterinary Medicine, Kangwon National University, Chuncheon-si 24341, Republic of Korea
[2]Department of Life Sports Educator, Kongju National University, Kongju 32588, Republic of Korea
[3]Platform Technology Group, Prestige Biopharma IDC, Busan 46726, Republic of Korea
[4]Central Research Institute, Designed Cells Co., Ltd, Cheongju 28576, Republic of Korea
[5]Laboratory of Veterinary Toxicology, College of Veterinary Medicine, Chungbuk National University, Cheongju-si 28644, Republic of Korea

*Corresponding authors. Dongsun Park, DVM, PhD, Laboratory of Veterinary Toxicology, College of Veterinary Medicine, Kangwon National University, 1 Kangwondaehak-gil, Chuncheon-si, Gangwon 24341, Republic of Korea. E-mail: dvmdpark@kangwon.ac.kr; Yun-Bae Kim, DVM, PhD, Laboratory of Veterinary Toxicology, College of Veterinary Medicine, Chungbuk National University, 1 Chungdae-ro, Seowon-gu, Cheongju-si, Chungcheongbuk-do 28576, Republic of Korea. E-mail: solar93@cbnu.ac.kr.
‡These authors contributed equally.

Abstract

Background: Cerebral palsy (CP), primarily caused by perinatal cerebral hypoxia and ischemia, is a devastating neurological disease in children characterized by motor, behavioral, and cognitive disorders. This study aimed to evaluate the therapeutic effects of amniotic membrane mesenchymal stem cell-derived exosome-rich conditioned medium (ERCM) in a CP model.
Methods: ERCM components were analyzed using enzyme-linked immunosorbent assay. Biodistribution was examined via fluorescence-labeled ERCM in both normal and CP induced animals. In vitro, the neuroprotective effects of ERCM against lipopolysaccharide and potassium cyanide-induced cytotoxicity were assessed in human neural stem cells and oligodendrocyte progenitor cells, focusing on apoptosis, inflammation, and oligodendrocyte differentiation. In vivo, ERCM was injected into CP-induced animals, followed by evaluation of antiapoptotic and anti-inflammatory signaling, motor and cognitive function, and white matter integrity.
Results: ERCM contained a broad array of growth factors and demonstrated enhanced retention in CP-affected brain regions. In vitro, ERCM significantly reduced apoptos is and inflammation, and promoted oligodendrocyte maturation via upregulation of Nkx2.2, CN Pase, and MBP. In vivo, ERCM treatment improved motor and cognitive performance, in hibited cell death and inflammatory responses, and increased expression of oligodendrocyte markers, including Nkx2.2, Olig2, CNPase, and MBP via increasing growth factor expression. Furthermore, ERCM attenuated demyelination in the corpus callosum, a region particularly vulnerable in CP.
Conclusion: ERCM confers therapeutic benefits in CP by preserving neural stem and oligodendrocyte progenitor cells, modulating apoptosis and inflammation, and enhancing oligodendrocyte differentiation. Accordingly, ERCM may present a good candidate as a CP therapeutic agent.

Key words: exosome; AMMSC; cerebral palsy; neural stem cells; oligodendrocyte; growth factor.

Graphical abstract

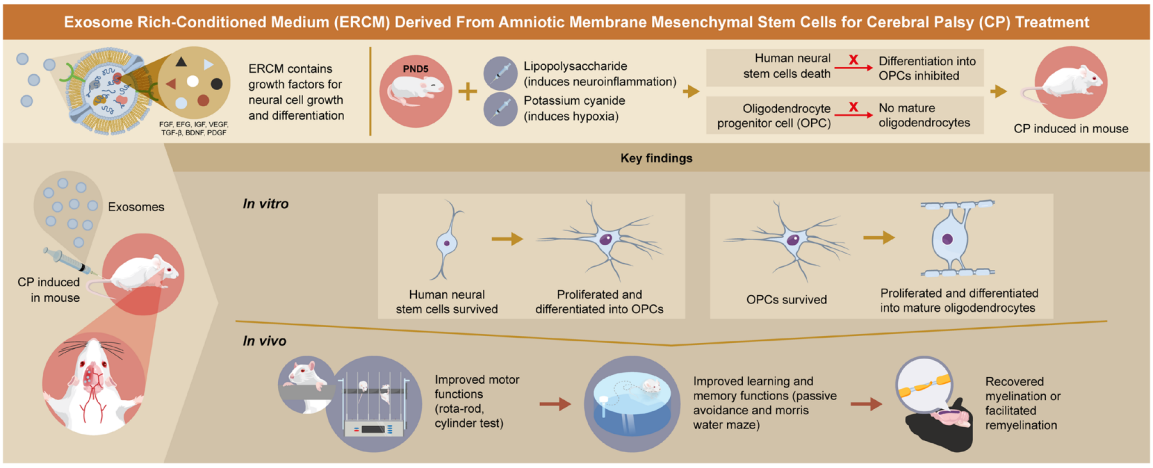

Received: 16 April 2025; Accepted: 12 November 2025.

Significance statement

The exosome-rich conditioned medium (ERCM) derived from amniotic membrane mesenchymal stem cells exerts potent neuroprotective and regenerative effects in a cerebral palsy model. Enriched with diverse growth factors and neurotrophic factors, ERCM promotes neural stem and oligodendrocyte progenitor cell survival, reduces inflammation, and enhances differentiation into mature oligodendrocytes. Through these mechanisms, ERCM markedly improves motor and cognitive function and preserves white matter integrity. These findings highlight ERCM as a promising therapeutic candidate for cerebral palsy and potentially other neurodevelopmental disorders characterized by inflammation and white matter injury.

Introduction

Cerebral palsy (CP) is a devastating neurological disease in children and is characterized by diverse neurobehavioral symptoms, including motor, perceptual, visual, behavioral, and cognitive dysfunctions.[1,2] The disease is also called periventricular leukomalacia, hypoxia-ischemia (HI), or white matter injury (WMI), depending on the lesion site.[3,4] Although the etiology may be multifactorial, intrauterine infection or asphyxia during delivery is a crucial etiological factor in many cases.[1] Respiratory dysfunction is a particularly predominant factor in preterm infants with a high CP incidence.[3,4] In addition, as the prevalence rate is expected to continually increase because of prenatal developments in medicine, developing therapeutic agents against CP is becoming increasingly urgent.[5]

Oligodendrocytes are crucial in CP.[4,6] Oligodendrocyte development begins with the differentiation of oligodendrocyte progenitor cells (OPCs) into immature oligodendrocytes that sheath axons and finally into myelin-producing oligodendrocytes.[7,8] In the human central nervous system, late preoligodendrocytes and immature oligodendrocytes are particularly susceptible to free radicals and inflammatory cytokines induced by HI insults and infection during the active myelination period (gestational weeks [GW] 24-40).[6,7,9–11] Therefore, in premature infants with CP, loss of myelin and delayed myelination by oligodendrocytes occur.[4,6]

Current therapeutic strategies are limited to supportive intensive care, such as clinical hypothermia.[12] Treatments with antioxidant, anti-inflammatory, and neuroprotective compounds, such as vitamin C (ascorbic acid), *N*-acetyl-l-cysteine, minocycline, and erythropoietin, attenuate WMI and delay physical dysfunction progression.[13,14] However, the effects of vitamin C, minocycline, and erythropoietin in animal models and humans remain controversial.[15–17] In addition, the relationship between the pathogenic mechanisms and factors of hypoxia-induced CP during delivery or intrauterine infection is unclear.

Therefore, therapeutic candidates for CP should prevent stem cell death and inflammation or free radical-induced oligodendrocyte damage and facilitate stem cell proliferation, oligodendrocyte differentiation into oligodendrocytes, and oligodendrocyte maturation to restore neurobehavioral function.[18,19] Various stem cells, such as mesenchymal stem cells, neural stem cells (NSCs), and multipotent progenitor cells have beneficial effects in HI brain injury.[2,14,20]

Exosomes have received considerable attention as therapeutic agents for neurological diseases owing to their biological functions. Exosomes are a subspecies of extracellular vesicles, approximately 30-150 nm in diameter, and are released into the extracellular fluid by cells in all living systems.[21] Exosomes contain cytokines, growth factors (GFs), signaling lipids, and genetic materials and are crucial in intercellular communication by transferring their materials between the source and target cells under physiological and pathophysiological conditions.[22] Exosome treatment improves neurobehavioral dysfunction in stroke and Alzheimer's disease models by exerting anti-inflammatory effects and promoting cell proliferation.[23,24]

Based on exosome function, we assessed the therapeutic effects of human amniotic membrane mesenchymal stem cell (AMMSC)-derived exosome-rich conditioned medium (ERCM) using a hypoxic culture process in human NSCs and OPCs under intrauterine infection or asphyxia and in CP-induced animals. We analyzed cell death inhibition, anti-inflammatory effects, and cell proliferation, differentiation, and maturation to oligodendrocytes as well as neurobehavioral function.

Methods

AMMSC preparation

AMMSCs were prepared under Good Manufacturing Practice conditions (Central Research Institute of Designed Cells Co., Ltd), as previously described.[25] Briefly, amniotic membrane tissues were digested with collagenase I (Sigma-Aldrich, St Louis), neutralized with an equal volume of medium containing 10% fetal bovine serum (FBS; Biowest), and centrifuged at 1500 × *g* for 10 minutes. After washing twice, the contaminated red blood cells (RBCs) were lysed with RBC lysis buffer, and the remaining cells were suspended in keratinocyte serum-free medium (Invitrogen) supplemented with 5% FBS, 100 U/mL penicillin, and 100 mg/mL streptomycin (Invitrogen). Cultures were maintained under 5% CO_2 at 37 °C in a culture flask. Media were changed every 2-3 days. The prepared amniotic stem cells were analyzed for their stem cell markers using flow cytometry. AMMSCs were confirmed to be mesenchymal and epithelial stem cells.[25]

ERCM collection

The separated amniotic membrane stem cells were suspended in the defined serum-free medium in Hyper flask (Nunc) and cultivated under normal oxygen (20% O_2, 5% CO_2) or hypoxic oxygen (2% O_2, 5% CO_2) conditions at 37 °C for 3 days. The media were filtered through a bottle-top vacuum filter system (0.22 μm; PES membrane) (Corning). The conditioned media were 30-fold concentrated using Vivaflow-200 (Sartorius).

Nanoparticle tracking analysis

The exosomes in the freeze-dried medium were analyzed using a NanoSight NS 300 instrument (NanoSight Ltd). The analysis settings were optimized and kept constant between samples, and the mean, mode, median, and estimated concentrations for each particle size were determined. As previously recorded,[24]

all analyses were performed with samples at a 1:1000 dilution, yielding particle concentrations in the region of 1.0×10^8 particles mL^{-1} (in accordance with the manufacturer's recommendations). All samples were analyzed in triplicate.

Bicinchoninic acid assay

The total protein concentration of the conditioned medium and ERCM was determined using the bicinchoninic acid (BCA) assay (Thermo Fisher Scientific) according to the manufacturer's instructions. Briefly, 2 µL of each sample or bovine serum albumin (BSA) standard was mixed with 200 µL of the working reagent in a 96-well plate and incubated at 60 °C for 30 minutes. After cooling to room temperature, the absorbance was measured at 562 nm using a microplate reader (SpectraMax, Molecular Devices). Protein concentrations were calculated from the standard curve generated using known concentrations of BSA.

CD9, CD63, and CD81 expression in ERCM

Protein-based quantification of CD9, CD63, and CD81 in the isolated exosomes was performed using a DC Protein Assay Kit (Bio-Rad Laboratories). Aliquots (25 µg) of normal conditioned medium (NCMs) and ERCM were denatured using 6× denaturation buffer at 95 °C for 10 minutes and resolved on 12% sodium dodecyl-sulfate-polyacrylamide gel by electrophoresis. The resolved proteins were transferred onto the Immobilon-P polyvinylidene fluoride membrane and blocked by incubation in 5% skim milk to minimize nonspecific antibody binding. Blocked blots were submerged with primary antibodies for CD9, CD63, and CD81 (1:1000; Abcam) overnight at 4 °C and subsequently washed thrice (10 minutes each) with ×1 Tris buffer saline with 0.1% Tween-20 (TBS-T) buffer followed by incubation with horseradish peroxidase (HRP)-conjugated secondary anti-mouse (1:2000; Abcam) antibodies for 2 hours at room temperature. Unbound antibodies were removed by washing with ×1 TBS-T buffer (3 × 10 minutes), and signals were recorded using the WestFemto Maximum Sensitivity Substrate Kit on a Bio-Rad ChemiDoc Imager (Bio-Rad Laboratories).

Enzyme-linked immunosorbent assay of growth factors and neurotrophic factors

The major GFs and neurotrophic factors (NFs) in AMMSC-NCM and AMMSC-ERCM were determined using enzyme-linked immunosorbent assay (ELISA), according to the manufacturer's instructions. Briefly, AMMSC-NCM or AMMSC-ERCM were placed inside the ELISA wells with antibodies specific for fibroblast growth factor (FGF) (ab219636; Abcam), epidermal growth factor (EGF) (ab217772; Abcam), insulin-like growth factor (IGF) (ab211652; Abcam), vascular epithelial growth factor (VEGF) (ab222510; Abcam), transforming growth factor-β (TGF-β) (ab100647; Abcam), and brain-derived neurotrophic factor (BDNF) (ab212166; Abcam) or platelet-derived growth factor (PDGF) (ab100622; Abcam) and incubated at room temperature for 0.5-1 hour. After washing 3 to 4 times with wash buffer, the primary antibodies were added, incubated at room temperature for 1 hour, and washed again. Secondary antibodies were treated and incubated at room temperature for 30-45 minutes, washed, and substrates were applied for 10-30 minutes to develop a color. After stopping color development using a stop solution, the absorbance was measured at 450 nm.

ERCM in vivo distribution in normal animal and CP animal models

The ERCM 1.0×10^{12} particles were incubated with ExoGlowTM-Vivo fluorescence dye 2 µL for 2 hours at room temperature. The mixture was filtered through a 15 cm column packed with Sepharose CL-6B to remove unlabeled free dye. Subsequently, fluorescence dye-labeled ERCM (4.5×10^{10} pn) was administered intravenously via the tail vein of normal and CP animal models. The organs were harvested according to time points, 0.25, 1, 2, 3, 5, and 24 hours, following the administration of labeled ERCM. Before collecting the brains, the whole body was perfused with phosphate-buffered saline (PBS) through the heart following complete anesthesia for 5 minutes. The harvested brains were analyzed for fluorescence intensity using the Vieworks, VISQUE In Vivo LF Smart in the near-infrared wavelength range (excitation at 784 nm and emission at 806 nm). The fluorescence intensity in the brains was expressed as radiant efficiency, which is a reliable intensity value.

Cell culture and treatment

Human NSC (F3) and OPC (F3.Olig2) were established as previously described.[19,26] The cells were cultured and maintained in the culture medium. The culture medium comprised Dulbecco's modified Eagle's medium (Biowest) fortified with antibiotics (100 IU/mL penicillin and 100 µg/mL streptomycin). The medium was further supplemented with 10% heat-inactivated FBS (Biowest). Cell cultures were incubated at 37 °C in an environment maintained at 5% CO_2 and 95% air. For all experiments, cells were grown until they reached >90% confluence and were ensured to be within their first 20 passages to maintain optimal growth conditions and genetic stability.

To investigate the protective effects of ERCM, F3, and F3.Olig2 cells were seeded in 10 cm dishes. After 24 hours of incubation, the cells were washed twice with PBS and treated with lipopolysaccharide (LPS) (10 µg/mL) or potassium cyanide (KCN) (5 µm) and ERCM (10, 30, and 100 µg/mL). The concentration of exosomes was measured using the BCA assay method (Thermo Scientific). The media were used to analyze lactate dehydrogenase (LDH) concentrations, and the cells were used for real-time polymerase chain reaction (PCR) and western blotting.

LDH assay in F3 and F3.Olig2 cells

The protective effect of ERCM was quantified by measuring LDH release from F3 and F3.Olig2 cells. LDH content was determined using a commercial nonradioactive LDH assay kit (Promega) based on a coupled enzymatic reaction that converts a tetrazolium salt into a red formazan product. Formazan was spectrophotometrically quantified by measuring the absorbance at 490 nm (Molecular Devices).

CP animal model

Nine-week-old pregnant Sprague–Dawley rats were purchased from Daehan Biolink (Eumseong). Rats were housed in an environmentally controlled room with a constant temperature

(23 ± 3 °C) and relative humidity (50% ± 10%), and a 12 hour-light/dark cycle. The rats were fed a standard rodent diet and purified water ad libitum. Neonates were obtained from natural delivery, and male pups of postnatal day (PND) 5 underwent hypoxia-ischemia-lipopolysaccharide injection (HIL); that is, their left common carotid artery was occluded and placed in a hypoxia incubator (H85 hypoxia workstation; Don Whitley Scientific) maintained at 8% O_2/92% N_2 condition for 2 hours. Finally, the sutures were removed for reperfusion, and the pups were intraperitoneally injected with LPS (1 mg/kg) after 0.5 hours of recovery to induce inflammation and returned to their dam. Control animals underwent only a sham operation (exposure of the left common carotid artery without occlusion) and vehicle treatment. The rats received the ERCM once at only PND7 in the single-dose groups (1.5×10^{10} and 6.0×10^{10}) or repeatedly at PND7, 17, 27, and 37 in the repeated-dose group (6.0×10^{10}) via the tail vein. All animal experiments were performed following the standard operating procedures of the Laboratory Animal Center, Chungbuk National University (CBNU), Korea. The study protocol was approved by the Institutional Animal Care and Use Committee of the CBNU (#CBNUA-1720-22-02).

Cylinder test

To evaluate forelimb use asymmetry owing to ipsilateral brain damage, the ratio of contralateral forelimb use was analyzed at PND10, 20, 30, and 40. Each animal was placed individually in a glass cylinder (21 cm in diameter and 34 cm in height) for 3 minutes. The weight-bearing forepaw in contact with the cylinder wall during full rearing was recorded as left (normal), right (impaired), or both. Paw preference was calculated as follows: [(normal forepaw – impaired forepaw)/(normal forepaw + impaired forepaw + both forepaws) × 100].

Rotarod performance

Motor balance and coordination were evaluated using a rotarod test system (Panlab Technology) at PND10, 20, 30, and 40. The speed of the rotarod was progressively increased: 2 rev/min at PND10, 10 rev/min at PND20, and 25 rev/min at both PND30 and PND40, and the time taken for the rats to fall off the rod was recorded. The average latency was calculated based on 3 consecutive measurements.

Passive avoidance performance

To evaluate memory acquisition, the rats were subjected to a shuttle box (ENV-010MD; Med Associates Inc.) once a day for 5 consecutive days from PND41. The shuttle-box apparatus comprises 2 light and dark compartments: a light chamber equipped with a lamp and a dark chamber with a steel grid floor for electric shock. During the trials, an electric shock (1 mA for 2 hours) was delivered when the rats entered the dark compartment from the light room through a guillotine door. The latency time in the light room was recorded during the 5-day trial. The endpoint was set at 300 hours, indicating the full acquisition of memory.

Morris water maze performance

To evaluate spatial memory, rats were subjected to the Morris water maze test (Smart v2.5; Panlab Technology). Water maze trials were performed in a circle water pool (180 cm in diameter) filled with water (27 cm in depth) maintained at 22 ± 2 °C. The pool was divided into 4 quadrants, and a hidden escape platform (10 cm in diameter and 25 cm in height) was submerged in the center of one quadrant, 2 cm below the surface of the water. The rats were subjected to 5 trials once a day from PND41 to find the platform hidden by white styrofoam granules (5 cm in diameter) on the surface of the water based on several external cues. The cue positions remained unchanged throughout the experiment. The escape latency (time taken to escape to the platform during the trials) was recorded.

Quantitative real-time PCR analysis

Total RNA was extracted from F3, F3.Olig2 cells, as well as from brain tissues obtained from the lesion-induced hemisphere of CP rats using TRIzol reagent (Invitrogen) following the manufacturer's instructions. Real-time quantitative PCR was performed as previously described.[27] The housekeeping gene, glyceraldehyde 3-phosphate dehydrogenase (GAPDH), served as an internal standard for normalizing target transcript expression. Primers used to amplify the transcripts of nuclear factor kappa B (NF-κB), tumor necrosis factor-α (TNF-α), interleukin-6 (IL-6), inducible nitric oxide synthase (iNOS), and cyclooxygenase2 (COX2) are listed in Table S1, Additional File 1. Data from three independent assays, each conducted in triplicate, were analyzed using the comparative Ct method.[27]

Western blotting

Proteins were extracted from cultured F3 and F3.Olig2 cells, as well as from brain tissues obtained from the lesion-induced hemisphere of CP rats. Samples were homogenized in 10 volumes of radioimmunoprecipitation assay buffer (Thermo Scientific) containing protease inhibitors (Sigma-Aldrich) and phosphatase inhibitors (Sigma-Aldrich). Western blotting was performed as previously described.[27] The membranes were immunoblotted with primary antibodies, followed by incubation with HRP-conjugated anti-rabbit and anti-mouse secondary antibodies (Jackson ImmunoResearch Laboratories Inc.). The antibodies used in this study are listed in Table S2, Additional File 1. Band densities were measured using the ImageJ software (version 1.53; National Institutes of Health) and normalized to the density of actin.

Luxol fast blue staining

At 45 days of age, rats were deeply anesthetized and euthanized by transcardial perfusion with PBS followed by 4% paraformaldehyde. Brains were removed, post-fixed in 4% paraformaldehyde for 48 hours, and cryoprotected in 30% sucrose solution for 72 hours at 4 °C. Coronal brain sections (10 μm thickness) were prepared using a cryostat and stained with Luxol Fast Blue (LFB) to evaluate myelin preservation. Images were acquired with an EVOS FL Auto2 Cell Imaging System (Thermo Fisher Scientific). The intensity of LFB staining was quantified using ImageJ software, and results were expressed as relative values compared to the normal group.

Immunostaining

The brain tissues of the rats were perfused with a 10% paraformaldehyde solution, followed by 48 hours of post-fixation in the same solution. Tissues were cryoprotected in a 30%

sucrose solution for 72 hours. Coronal cryosections, 1.0 mm posterior to the bregma and 10 μm thick, were prepared. For immunohistochemical staining, cryosections were rinsed in TBS and treated with 3% hydrogen peroxide for 5 minutes to block endogenous peroxidase activity. After rinsing with TBS and a blocking step with 5% BSA, the sections were incubated at 4 °C overnight with a PDGFR-specific antibody (1:300; rabbit polyclonal, Chemicon). This was followed by incubation with a secondary antibody conjugated with Alexa Fluor-594 (1:300; Molecular Probes). For double immunostaining, sections were incubated with anti-Sox10 and Olig2 as primary antibodies. A secondary antibody conjugated with Alexa Fluor-488 (1:200; Molecular Probes) was used for the procedures, the same as PDGFR staining. The sections were counterstained with 4′,6-diamidino-2-phenylindole (Sigma-Aldrich) for nuclei visualization. Following staining, all samples were photographed using a fluorescence microscope (EVOS FL Auto2 Cell imaging system).

Statistical analysis

Statistical comparisons between groups were performed using a 1-way analysis of variance, followed by Tukey's multiple comparison test for multigroup data. For two-group comparisons, the unpaired Student's *t*-test was applied. All analyses were conducted using the Statistical Package for Social Sciences for Windows (version 12.0; SPSS Inc.). Statistical significance was set at $P < .05$. All data are expressed as the mean ± standard deviation (SD).

Results

Exosome characteristics in NCMs and ERCM

The contents and numbers of exosomes in NCMs and ERCM were measured based on exosome marker expression, such as CD9, CD63, and CD81, and nanoparticle tracking analysis (NTA), respectively. The levels of CD9-, CD63-, and CD81-positive exosomes were significantly lower in NCMs obtained under normoxic conditions (20% O_2) than in ERCM collected after hypoxic culturing (2% O_2) (Figure 1A).

The particle number of exosomes in NCM and ERCM was 9.0×10^8/mL and 4.5×10^{10}/mL, respectively (Figure 1B). Thus, the number of exosomes in ERCM increased up to 50 times that in NCMs. In addition, BCA protein quantification revealed that the protein concentration of ERCM was 5.55 ± 0.10 μg/mL, whereas NCM showed 0.1536 ± 0.04 μg/mL, indicating a nearly 40-fold increase in total protein content in ERCM. The mean size of the exosomes in the major peak from AMMSCs was 68 nm (Figure 1C); however, several small peaks were also found, which might be attributable to exosome aggregation.

FGF, EGF, IGF, VEGF, TGF-β, BDNF, and PDGF concentrations, that is, GFs and NFs related to cell protection, proliferation, and differentiation, were significantly low in NCM. In comparison, the GFs and NFs were significantly high in the ERCM, reaching 10 to 100 times that in the NCM (Figure 1D).

Characterization of conditioned media showed that ERCM contained higher numbers of particles and greater amounts of growth and NFs compared with NCM. Therefore, ERCM was used for subsequent cell-based assays and in vivo experiments to evaluate its therapeutic efficacy. To investigate lesion tropism, exosomes were labeled with a fluorescent dye and injected into normal and CP-induced animals via the tail vein. In normal animals, the intensity of the exosomes peaked at 3 hours and decreased thereafter (Figure 1E). In comparison, in CP-induced animals, the fluorescence intensity increased at 2 hours and then decreased. The fluorescence intensity was higher in CP-induced animals (Figure 1H) than in normal animals (Figure 1G), and the area under the curve of CP-induced animals was more than twice that of normal animals (Figure 1F).

Protective effect of ERCM in LPS- or KCN-damaged human NSCs

To induce CP, NSCs were treated with LPS (intrauterine infection) or KCN (hypoxic conditions), and the protective effects of ERCM were evaluated. In F3 cells, LPS treatment (10 μg/mL) increased LDH release, whereas ERCM treatment (10, 30, and 100 μg/mL) significantly reduced LDH release in a concentration-dependent manner (Figure 2A). In addition, ERCM treatment exerted anti-inflammatory effects. In F3 cells, LPS treatment significantly upregulated NF-κB expression (Figure 2B). NF-κB expression was markedly attenuated by ERCM treatment. Similar to the change in NF-κB expression, that of TNF-α and IL-6 was also significantly increased by LPS, which was blocked by treatment with ERCM (Figure 2C and D). Similarly, inflammatory enzyme expression of iNOS and COX2 increased following LPS exposure; LPS regulated the expression of pro-inflammatory proteins, such as iNOS and COX2 (Figure 2E and F). ERCM treatment significantly inhibited the expression of these enzymes in a concentration-dependent manner.

Similarly, KCN (5 μm) significantly increased LDH release from F3 cells; however, ERCM treatment significantly decreased it in a dose-dependent manner (Figure 2G). In addition, in mRNA expression of inflammatory mediators, KCN significantly increased NF-κB, TNF-α, IL-6, iNOS, and COX2 expression (Figure 2H-L). However, treatment with ERCM significantly inhibited the expression of these genes.

Western blotting revealed that proteins related to apoptosis, such as Bax, were upregulated by LPS or KCN treatment, whereas Bcl-2 was downregulated. However, the damage caused by LPS or KCN was markedly attenuated by ERCM treatment, although sensitivities differed (Figure 2M-T). Notably, treatment with ERCM upregulated cell proliferation-related protein expression, such as AKT and PI3K, as well as oligodendrocyte differentiation-related proteins, such as PDGFR A, SOX10, Nkx2.2, and Olig2.

Protective effect of ERCM in LPS- or KCN-damaged human OPCs

To investigate the protective effect of ERCM in OPCs, ERCM (10, 30, and 100 μg/mL) was administered to LPS- (10 μg/mL) or KCN (5 μm)-damaged F3.Olig2 cells. As with F3 cells, ERCM treatment significantly reduced LDH release in LPS- or KCN-damaged F3.Olig2 cells (Figure 3A and G). Similarly, ERCM treatment significantly reduced inflammatory indicator expression such as NF-κB, TNF-α, IL-6, iNOS, and COX2, which were increased by LPS or KCN treatment (Figure 3B-F and H-L). Regarding protein expression, ERCM treatment attenuated apoptosis in KCN- or LPS-damaged F3.Olig2 cells and facilitated cell proliferation and differentiation (Figure 3M-T). ERCM treatment significantly increased

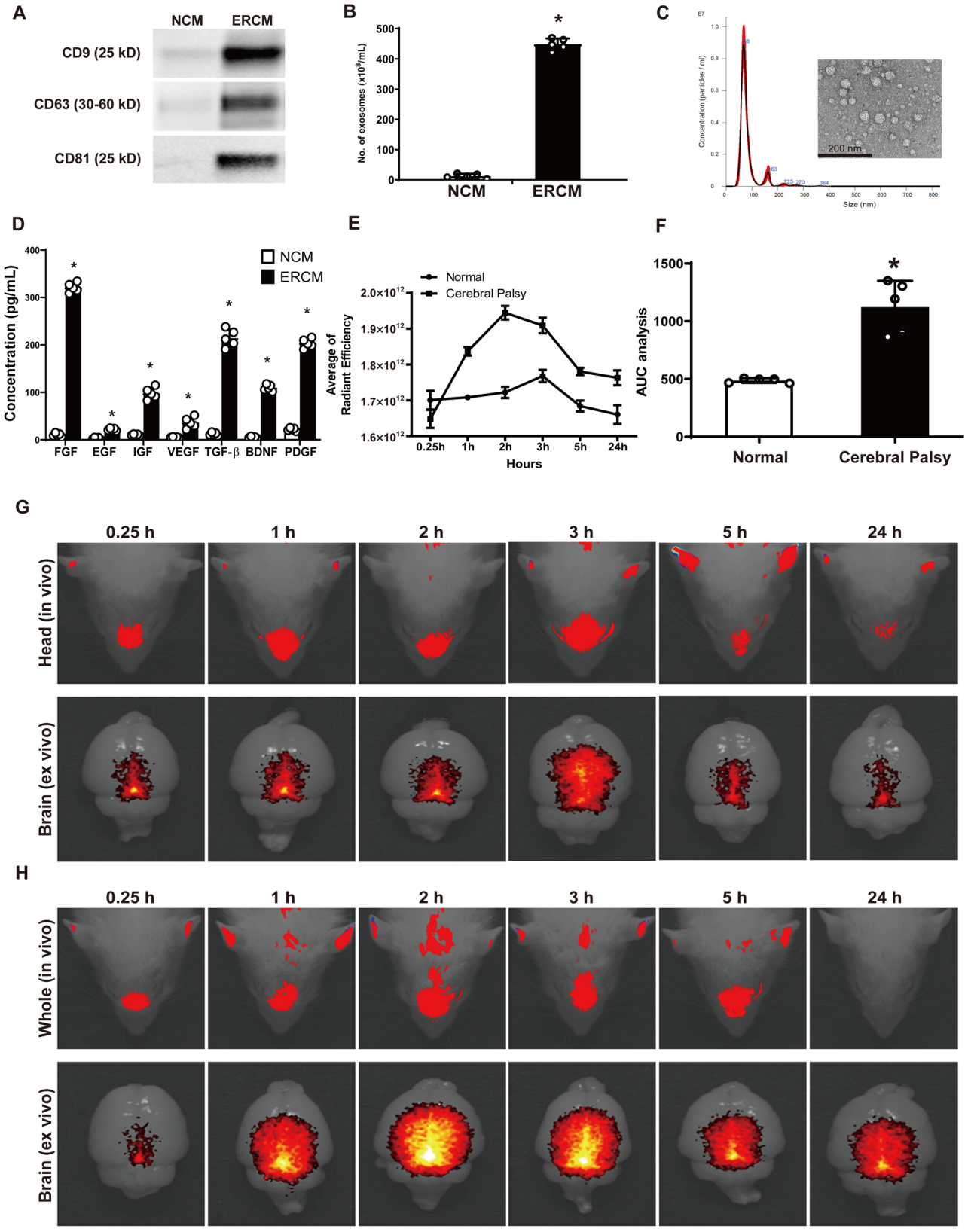

Figure 1. Characteristics of exosome-rich conditioned medium (ERCMs) obtained from amniotic membrane mesenchymal stem cells (AMMSCs). (A) Contents of CD9, CD63, and CD81-positive exosomes in normal conditioned medium (NCM) and ERCM. (B) Number of exosomes in NCM and ERCM. (C) Particle size distribution of AMMSC exosomes. (D) Concentrations of growth factors and neurotrophic factors in NCM (white bars) and ERCM (black bars) of AMMSCs. (E) Intensity of radiant efficiency of fluorescence-labeled exosomes into normal and cerebral palsy-induced animal. (F) AUC analysis of radiant efficiency. (G and H) In vivo image of fluorescence intensity at 0.25, 1, 2, 3, 5, and 24 hours in normal animal (G) and cerebral palsy-induced animal (H). FGF, fibroblast growth factor; EGF, epidermal growth factor; IGF, insulin-like growth factor; VEGF, vascular endothelial growth factor; TGF-β, transforming growth factor-β; BDNF, brain-derived neurotrophic factor; PDGF, platelet-derived growth factor. All comparisons were analyzed using an unpaired, 2-tailed Student's *t*-test (mean ± SD). *Significantly different from each NCM ($P < .05$).

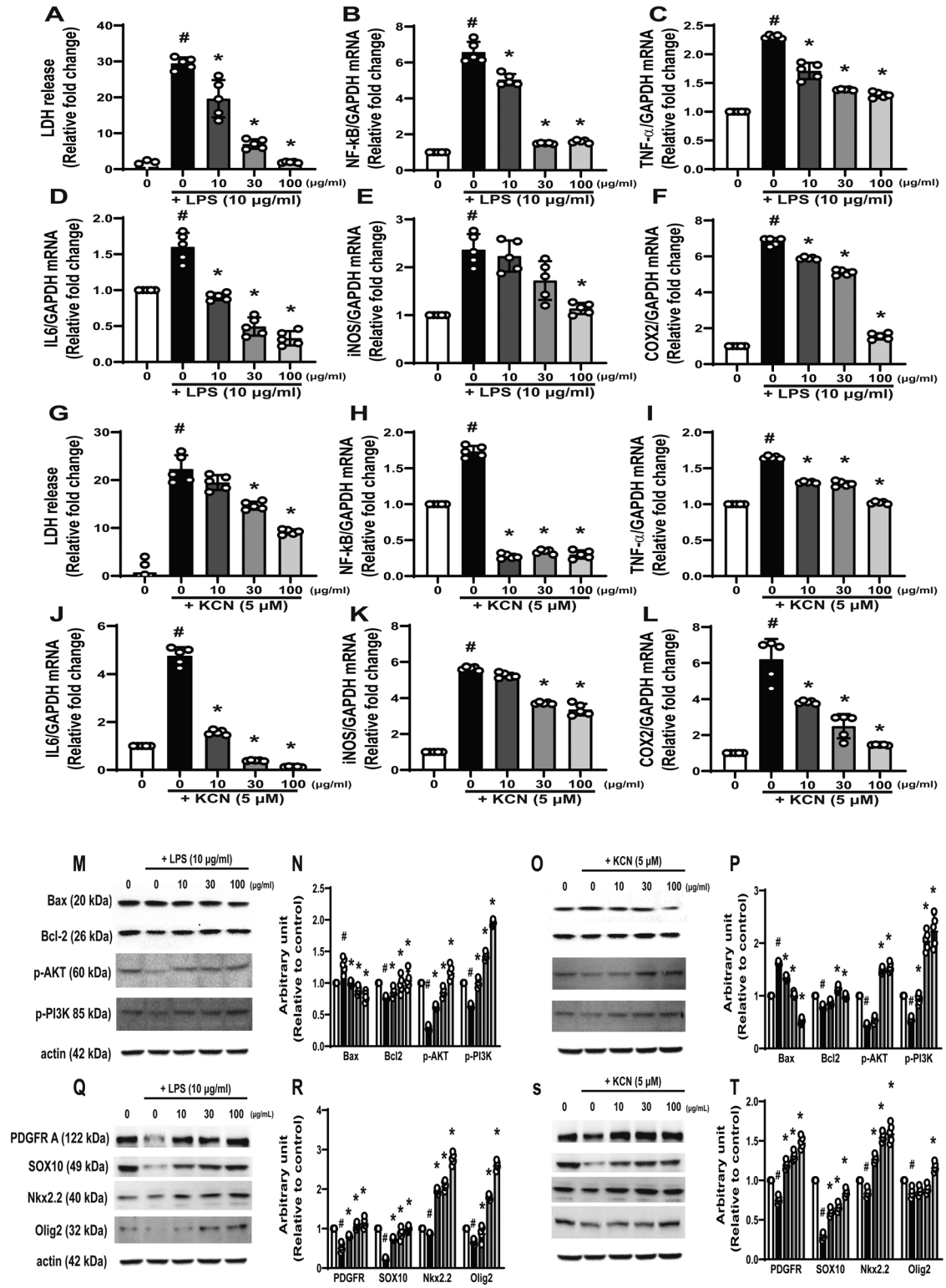

Figure 2. Protective effect of ERCM in human neural stem cells (F3 cells) damaged by LPS or KCN. (A) The protective effects of ERCM (10, 30, and 100 μg/mL) treated with LPS (10 μg/mL) in the lactate dehydrogenase (LDH) assay. (B-F) Real-time polymerase chain reaction (PCR) analysis of mRNA of nuclear factor (NF)-κB (B), tumor necrosis factor (TNF)-α (C), interleukin (IL)-6 (D), inducible nitric oxide synthase (iNOS) (E), and cyclooxygenase 2 (COX2) (F) normalized to glyceraldehyde-3-phosphate dehydrogenase (GAPDH). (G) The protective effects of ERCM (10, 30, and 100 μg/mL) treated by KCN (5 μm) in the LDH assay. (H-L) Real-time PCR analysis of the mRNA of NF-κB (H), TNF-α (I), IL-6 (J), iNOS (K), and COX2 (L). (M-S) Western blotting of Bax, Bcl-2, p-AKT and p-PI3K, PDGFR A, Sox10, Nkx2.2, and Olig2 damaged by LPS (M, Q) and KCN (O, S) and band densities normalized to actin (N, P, R, and T). Densitometric analysis of western blotting was performed using ImageJ. $n = 5$ per treatment group. One-way ANOVA with Tukey's multiple-comparison test (mean ± SD). #Significantly different from normal control ($P < .05$). *Significantly different from vehicle control ($P < .05$).

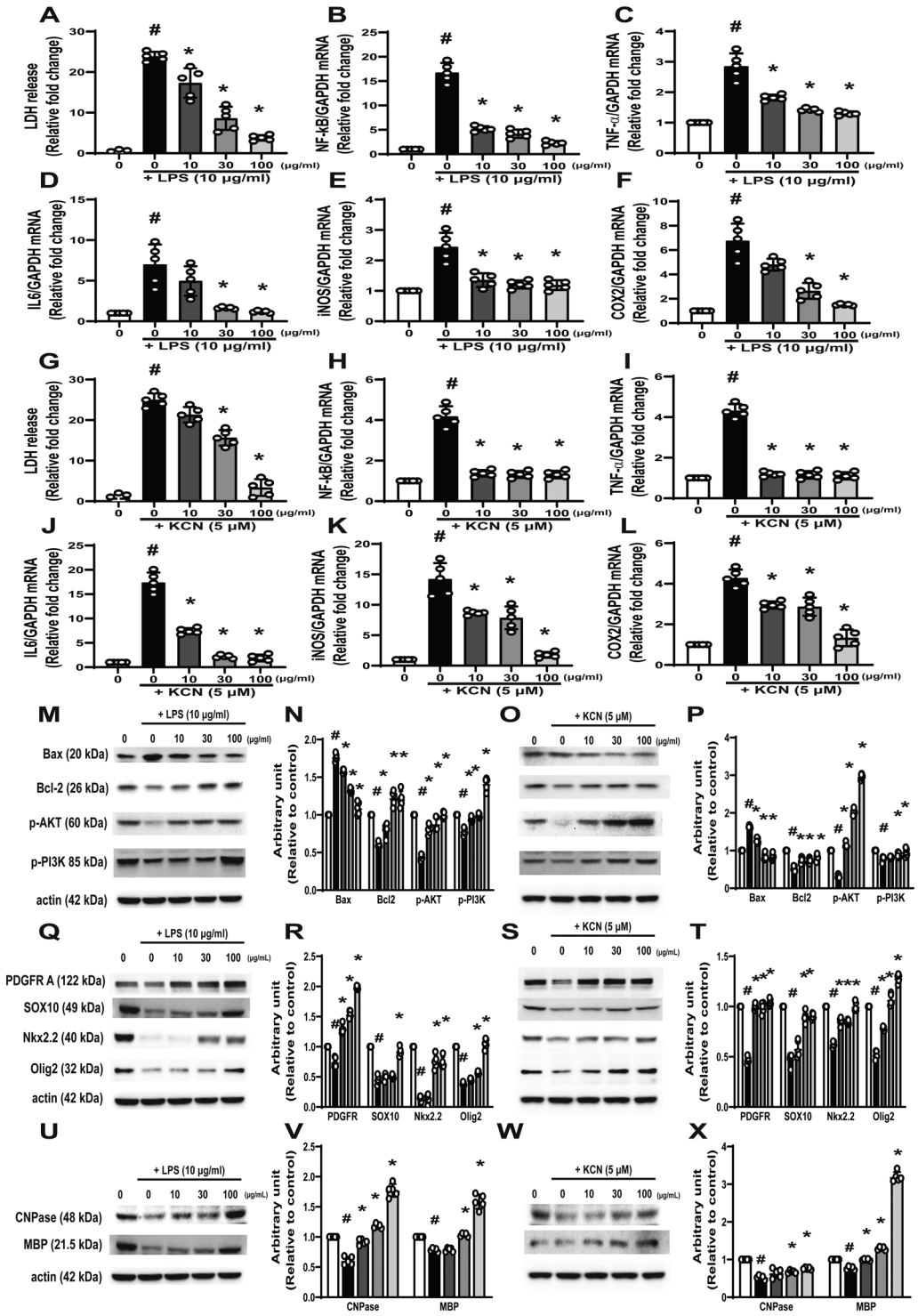

Figure 3. Protective effect of ERCM in human oligodendrocyte progenitor cells (F3.Olig2 cells) damaged by LPS or KCN. (A, G) The protective effects of ERCM (10, 30, and 100 μg/mL) treated with LPS (A) and KCN (G) in the LDH assay. (B-F, H-L) Real-time PCR analysis of the mRNA of NF-κB (B, H), TNF-α (C, I), IL-6 (D, J), iNOS (E, K), and COX2 (F, L) normalized to GAPDH; upper panel (B-F) is damaged by LPS and lower panel (H-L) is damaged by KCN. (M-X) Western blotting of Bax, Bcl-2, p-AKT and p-PI3K, PDGFR A, Sox10, Nkx2.2, Olig2, CNPase, and MBP damaged by LPS (M, Q, and U) and KCN (O, S, and W) and band densities normalized to actin (N, P, R, T, V, and X). Densitometric analysis of western blotting was performed using ImageJ. $n = 5$ per treatment group. One-way ANOVA with Tukey's multiple-comparison test (mean ± SD). #Significantly different from normal control ($P < .05$). *Significantly different from vehicle control ($P < .05$).

oligodendrocyte maturation markers, such as CNPase and MBP (Figure 3U-X).

Therapeutic effect of ERCM in CP-induced animal model

To investigate the therapeutic effect of ERCM, the rats were subjected to HIL at PND5, and received ERCM doses once at only PND7 in the single-dose groups (1.5×10^{10} and 6.0×10^{10}) or repeatedly at PND7, 17, 27, and 37 in the repeated-dose group (6.0×10^{10}) via the tail vein. In the cylinder test, normal animals used their left and right forelimbs in similar ratios at PND10, 20, 30, and 40 (Figure 4A). However, rats subjected to HIL at PND5 showed significantly decreased (<30%) use of the forelimb contralateral to the brain injury at PND20, 30, and 40. This reduced use of the contralateral forelimb was recovered to near-normal levels by a single injection of ERCM on PND7. A similar restoration of physical dysfunction of the contralateral forelimb induced by HIL was achieved with repeated injections of ERCM at PND7, 17, 27, and 37.

The latency time of the sham control animals on the rotarod gradually increased according to their growth from a mean of 6.5 hours at PND10 to 30 hours at PND40 (Figure 4B). However, HIL caused the impairment of motor function and coordination, leading to a significant reduction in the latency time (3 hours at PND10 and 5 hours at PND20-40). This decreased rotarod performance was restored at PND20-40 by the injection of ERCM. Particularly, the functional impairments in CP-induced rats were significantly near-fully recovered following repeated ERCM injections.

Hypoxia-ischemia-lipopolysaccharide injection at PND5 induced severe impairment of learning and memory functions, assessed using passive avoidance and Morris water maze performances at PND41-45. CP-induced rats displayed a significantly delayed increase in retention time and long latency time during repeated trials in passive avoidance and Morris water maze performances, respectively, whereas full memory acquisition was completed in normal animals (Figure 4C-E). In comparison, injection of ERCM once at PND7 or four times at PND7, 17, 27, and 37 significantly recovered impaired learning and memory function in passive avoidance trials. In addition, ERCM injection improved cognitive dysfunction, and the effect of repeated injections was superior to that of a single injection.

As in the cell experiment, inflammatory indicators, such as NF-κB, TNF-α, IL-6, iNOS, and COX2, were significantly increased in the CP-induced animals compared with those in normal animals, and they were significantly reduced by ERCM injection (Figure 5A-E). The effect of repeated injections was superior to that of single injections.

Similarly, western blotting showed that Bax expression was increased by HIL, whereas Bcl-2 expression was decreased. However, these effects were reversed by ERCM injection (Figure 5F and G). In addition, the ERCM-treated group showed significantly increased levels of cell proliferation markers, such as p-AKT and p-PI3K. In the CP-induced group, the differentiation and maturation markers for oligodendrocytes were decreased by HIL and increased by the injection of ERCM (Figure 5J, K, N, and O). Furthermore, GFs and NFs, such as NT3, NGF, BDNF, CNTF, GDNF, and PDGF A and B, were significantly increased by ERCM injection (Figure 5H, I, L, and M). The effect of repeated injections was superior to that of single injections.

Myelin assessment and immunostaining

After LFB staining, myelin expression levels in the subventricular zone in the CP-induced group were significantly lower than that in the normal group (Figure 6A and B). The positive area in the corpus callosum particularly diminished. However, the positive areas were restored with ERCM injection. Repeated injections were the most effective.

To confirm whether ERCM injection increased PDGFR and their differentiation and maturation to oligodendrocytes, PDGFR (red), SOX10 (green, Figure 7A), and Olig2 (green, Figure 7B) were double-immunostained. Immunostaining showed that the number of PDGFR-positive cells was decreased by HIL in the corpus callosum area (Figure S1, see online supplementary material for a color version of this figure); however, the signals increased with ERCM injection (Figure 6C and D). In addition, PDGFR-positive cells showed intense SOX10 and Olig2 positive signals (Figure 6C and D).

Discussion

AMMSC-derived ERCM contain numerous exosomes and high concentrations of GFs and NFs under hypoxic conditions. Functionally, ERCM protected human NSCs and OPCs against LPS- and KCN-induced damage in vitro and restored myelin expression and neurobehavioral function in CP-induced animals.

Nanoparticle tracking analysis showed that AMMSC-derived ERCM had an average size of 68 nm, significantly smaller than that of exosomes derived from other stem cells,[28] which may facilitate penetration across biological barriers such as the blood-brain barrier (BBB). In a previous study, CM-DiI-labeled exosomes readily penetrated the intact and H_2O_2-injured pRGCs,[28] and in our study, fluorescence-labeled exosomes were readily distributed in the brains of normal and CP-induced animals. Notably, fluorescence intensity and retention time were increased in CP brains, likely due to BBB disruption caused by HIL and the lesion tropism of exosomes.[29]

For in vivo experiments, we employed the neonatal hypoxia–ischemia-induced CP model in PND5 rats, a developmental stage corresponding to gestational weeks 24-30 in humans, when oligodendrocytes are highly vulnerable and myelination has not yet fully commenced.[6,30] This model reflects well-recognized etiological factors of human CP, including intrauterine infection and perinatal complications, and reliably reproduces oligodendrocyte loss, impaired myelination, and motor deficits, consistent CP pathology.[31] Although variability in lesion severity is inherent, such heterogeneity mirrors the clinical situation, where CP patients also present with diverse neuropathology.[32] In our experiments, consistent findings such as oligodendrocyte loss and neurobehavioral impairments were observed, supporting the suitability of this model for evaluating the therapeutic potential of ERCM.[33] Importantly, ERCM injection substantially attenuated behavioral and cognitive dysfunction, with contralateral forelimb improvement observed within 4 days and maintained for more than 5 weeks.

The rationale for using exosomes is based on their functional molecules, including GFs and NFs, that promote cell proliferation and tissue protection.[24,28] Our ELISA results confirmed that

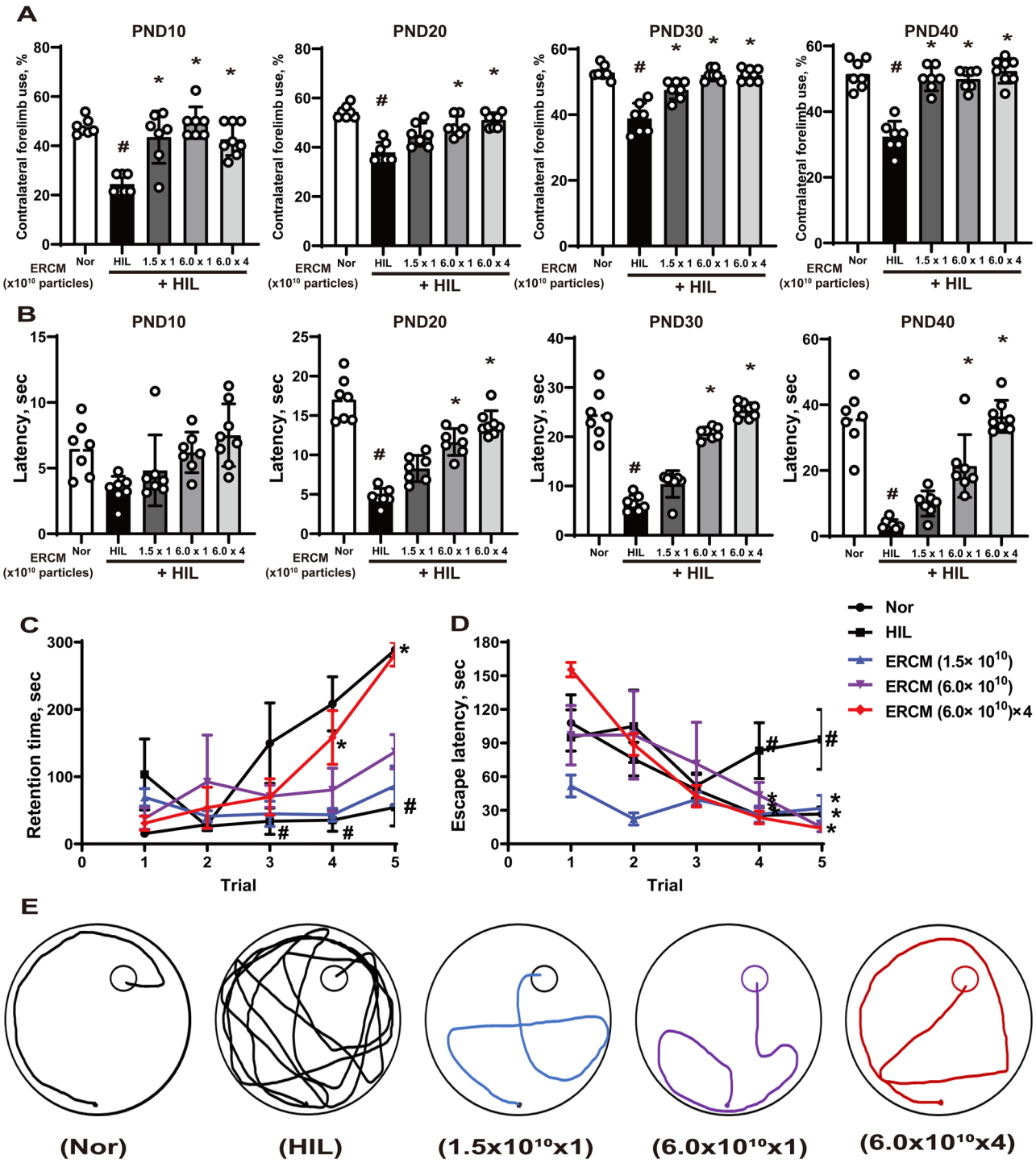

Figure 4. Therapeutic effect of ERCM on behavioral functions in cerebral palsy animal model. (A) Use ratio (%) of forelimb contralateral to hypoxia-ischemia-lipopolysaccharide injection (HIL) in the cylinder test at postnatal day (PND) 10, 20, 30, and 40. Rats ($n = 7$ per group) were subjected to HIL, and injected ERCM once at only PND7 in the single-dose groups (1.5×10^{10} and 6.0×10^{10}), or repeatedly at PND7, 17, 27, and 37 in repeated-dose group (6.0×10^{10}) via the tail vein. (B) Latency time (s) in rotarod performance at PND10, 20, 30, and 40. The speed of the rotarod was progressively increased: 2 rpm at PND10, 10 rpm at PND20, and 25 rpm at both PND30 and PND40. (C) Passive avoidance test and (D) Morris water maze test were conducted once daily from PND41 to PND45 to assess learning and memory functions. (E) Representative tracking images in the Morris water maze test. One-way ANOVA with Tukey's multiple-comparison test (mean ± SD). #Significantly different from normal control ($P < .05$). *Significantly different from vehicle control ($P < .05$).

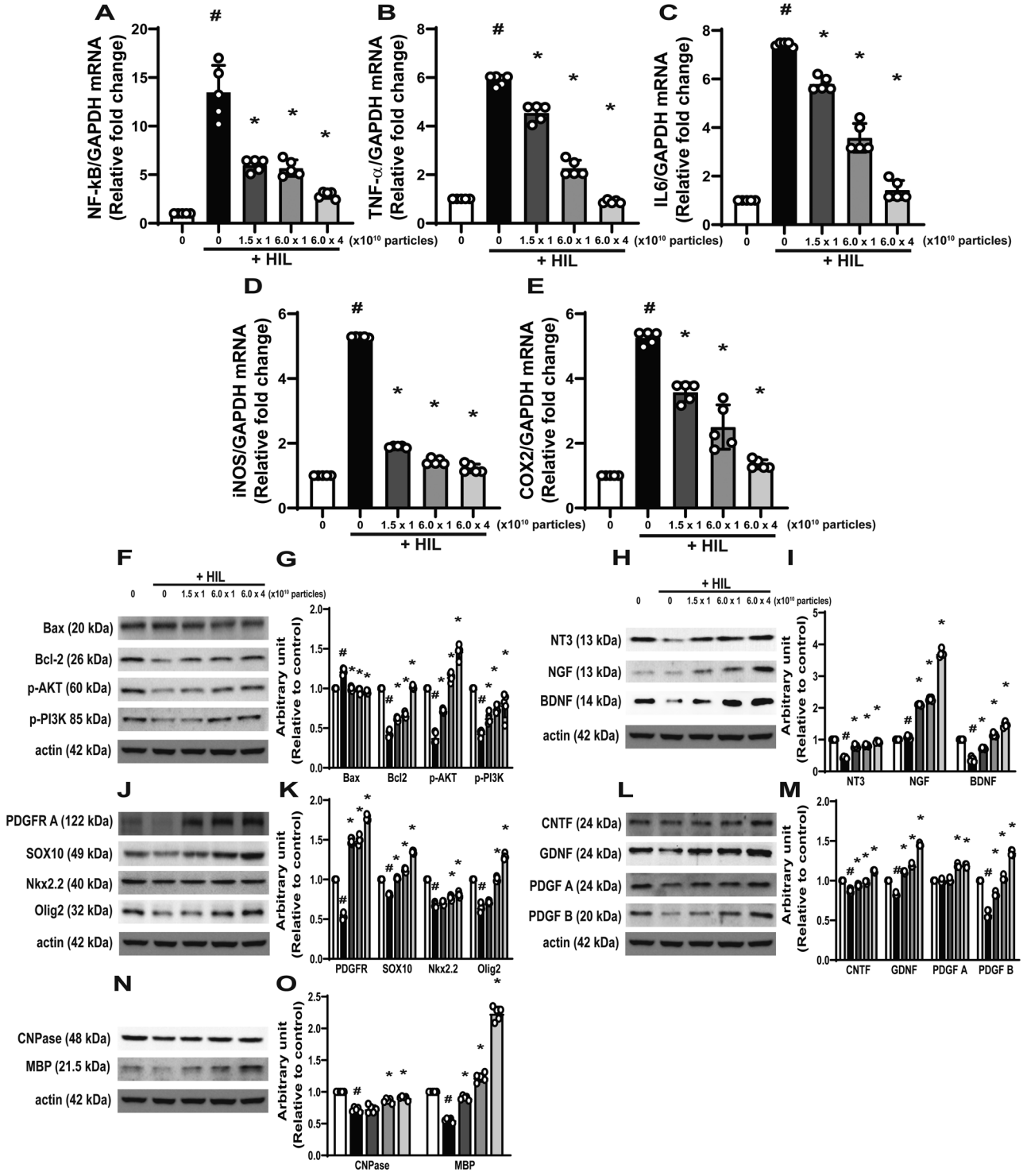

Figure 5. Therapeutic effect of ERCM on neuroinflammation and regeneration in the cerebral palsy animal model. (A-E) Real-time PCR analysis of mRNA of NF-κB (A), TNF-α (B), IL-6 (C), iNOS (D), and COX2 (E) normalized to GAPDH. (F-O) Western blotting of Bax, Bcl-2, p-AKT and p-PI3K, PDGFR A, Sox10, Nkx2.2, Olig2, CNPase, MBP, NT3, NGF, BDNF, CNTF, GDNF, PDGF A and B in brain tissues from the lesion-induced hemisphere of each group, and band densities normalized to actin (G, I, K, M, and O). Densitometric analysis of the Western blot was performed using ImageJ. $n = 5$ per treatment group. One-way ANOVA with Tukey's multiple-comparison test (mean ± SD). #Significantly different from normal control ($P < .05$). *Significantly different from vehicle control ($P < .05$).

ERCM contained higher levels of these trophic factors than NCM, correlating with protection against LPS- and KCN-induced damage in F3 and F3.Olig2 cells. Exosomes also carry thousands of additional molecules including GFs, NFs, miRNAs, cytokines, and other proteins,[34] that exert combinational and synergistic effects on cytoprotection, regeneration, anti-inflammation, and immune modulation. Our study provides novel evidence that ERCM derived from amniotic membrane MSCs enhances oligodendrocyte differentiation and survival in vitro and preserves white matter integrity in vivo, thereby linking cellular mechanisms with behavioral recovery. While the precise molecular pathways remain to be fully elucidated, these findings highlight the unique contribution of ERCM and its potential as a promising therapeutic strategy for CP.

Several studies have reported that exosomes derived from human amniotic or umbilical cord MSCs exert neuroprotective effects in CP models by attenuating apoptosis and promoting neuronal survival.[35,36] However, these studies primarily focused on purified exosomes, which represent only a subset of the paracrine components secreted by MSCs. In contrast, our study utilized ERCM derived from hypoxia-preconditioned amniotic membrane MSCs, which contains not only exosomes but also a broad spectrum of trophic and signaling molecules. This unique composition enhances oligodendrocyte maturation, remyelination, and neuroregeneration, extending beyond the anti-apoptotic effects described previously. Furthermore, hypoxic preconditioning significantly augmented the levels of NFs (VEGF, BDNF, NGF, and CNTF), thereby conferring superior therapeutic efficacy and translational potential compared with normoxic or single-factor approaches.

Hypoxic preconditioning likely further enriched the MSC secretome by upregulating trophic mediators such as VEGF, BDNF, and HGF, which are closely associated with neuroprotection and regeneration.[37,38] Although we did not perform comprehensive proteomic profiling, our ELISA data demonstrated elevated levels of representative GFs and NFs in ERCM, supporting the hypothesis that hypoxia contributed to the enhanced therapeutic efficacy of ERCM.

Mechanistically, ERCM treatment increased p-AKT and p-PI3K expression, consistent with activation of a signaling

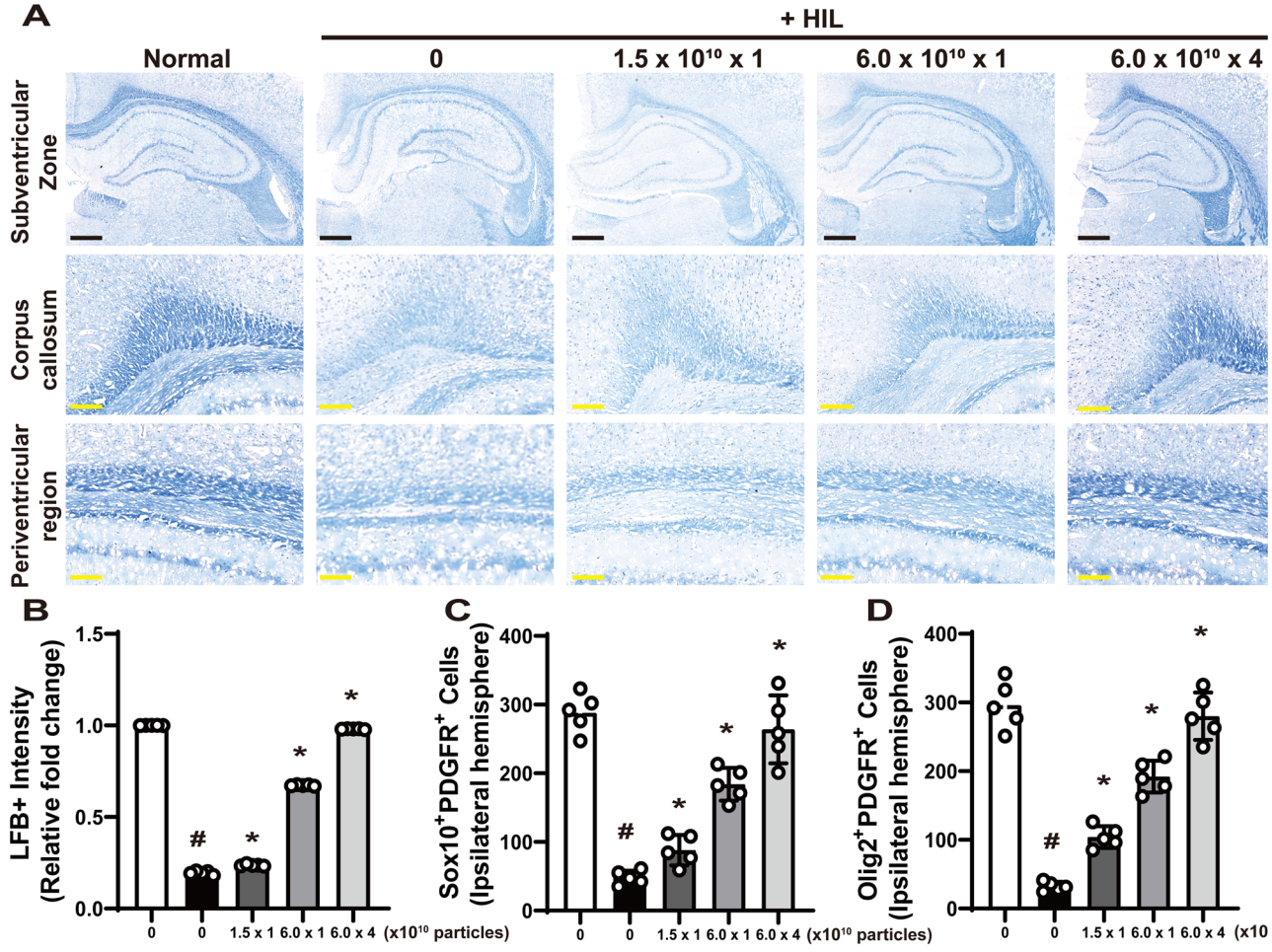

Figure 6. Therapeutic effect of ERCM on myelination and oligodendrogenesis in the cerebral palsy animal model. (A) Representative photomicrographs of myelin using Luxol Fast Blue (LFB) staining in the subventricular zone of PND45 rat brain. Rats ($n = 7$ per group) were subjected to HIL, and injected ERCM once at only PND7 in the single-dose groups (1.5×10^{10} and 6.0×10^{10}), or repeatedly at PND7, 17, 27, and 37 in repeated-dose group (6.0×10^{10}) via tail vein. Black scale bar = 1000 μm; yellow scale bar = 200 μm. (B) Quantification of LFB-positive intensity using ImageJ software. Values are expressed as relative intensity compared to normal control. (C, D) Quantification of Sox10⁺/PDGFRα⁺ (C) and Olig2⁺/PDGFRα⁺ (D) double-positive cells in the lesion-induced side of the brain. One representative region per section was analyzed for each animal. One-way ANOVA with Tukey's multiple-comparison test (mean ± SD). #Significantly different from normal control ($P < .05$). *Significantly different from vehicle control ($P < .05$).

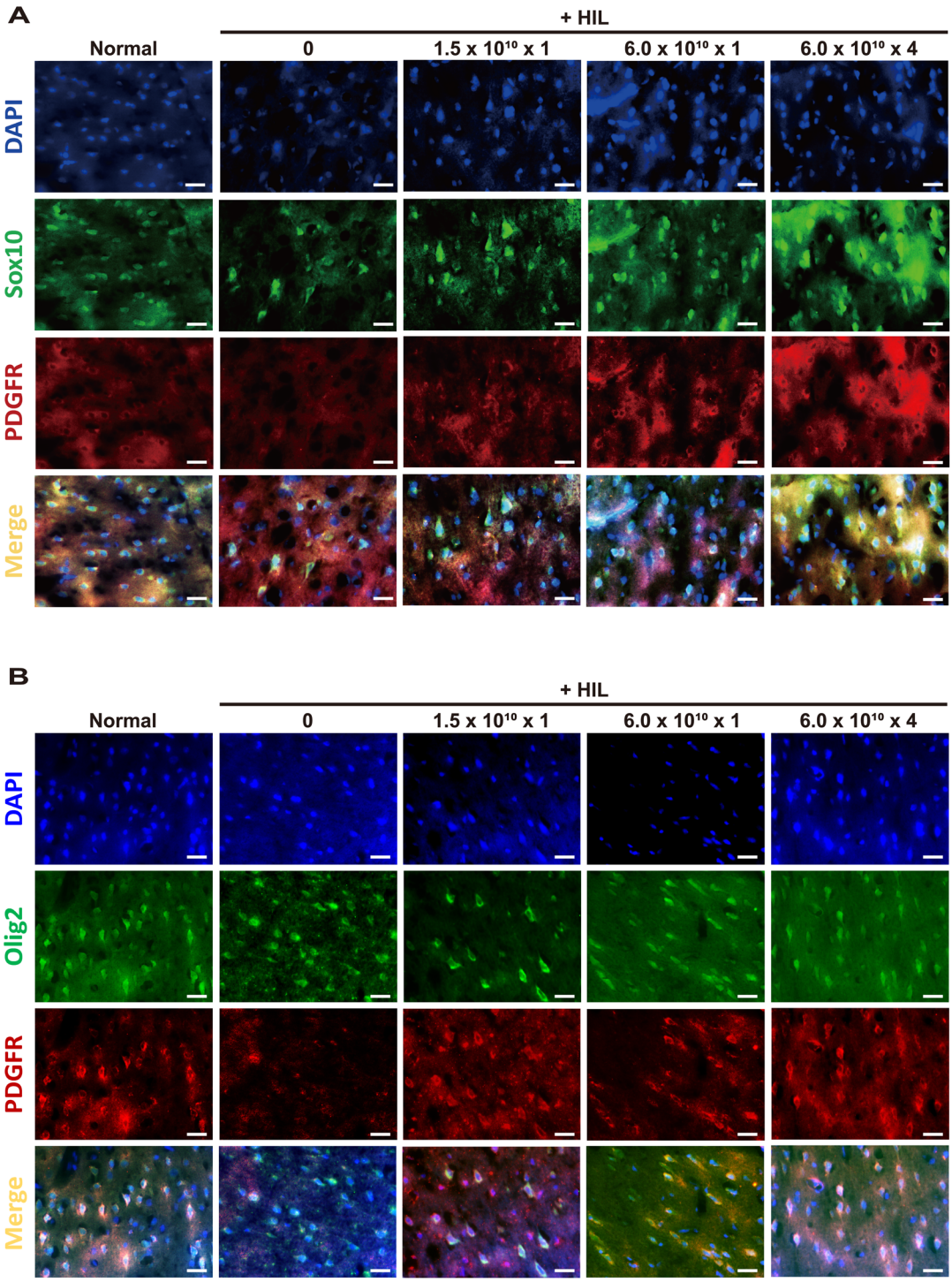

Figure 7. Representative immunohistochemistry images of oligodendrocyte lineage markers in the subventricular zone of the PND45 rat brain. (A) Double immunostaining of Sox10 (green) and PDGFRα (red), with DAPI (blue) as a nuclear counterstain. (B) Double immunostaining of Olig2 (green) and PDGFRα (red), with DAPI (blue). All images were obtained from the lesion-induced hemisphere. Scale bar = 20 μm.

pathway critical for neuroprotection and regeneration.[39] Although sustained activation of the PI3K/AKT pathway is implicated in tumorigenesis, in the nervous system this pathway is well known to promote neuronal survival, oligodendrocyte proliferation, and remyelination, while suppressing apoptosis. In our study, the observed upregulation of p-AKT and p-PI3K is most likely transient, beneficial pro-survival signaling that facilitated recovery in the CP model, rather than oncogenic activation. This interpretation is supported by the absence of tumor formation during the experimental period.

ERCM also promoted oligodendrocyte differentiation through PDGF-mediated signaling. PDGF is essential for activating SOX10 and Olig2, thereby driving NSC differentiation into oligodendrocytes.[40] PDGF binds to its receptor to activate

SOX10, which increases Olig2 expression [41,42] and promotes the differentiation of stem cells into oligodendrocytes. Consistent with this, ERCM was found to contain a significant amount of PDGF, and expression of PDGFR, SOX10, Nkx2.2, and Olig2 increased in a concentration-dependent manner in LPS- and KCN-damaged F3 and F3.Olig2 cells. Furthermore, ERCM enhanced the expression of oligodendrocyte maturation markers such as CNPase and MBP, confirming its role in promoting oligodendrocyte lineage progression.

In LFB staining, ERCM injection markedly preserved host myelin in CP-induced rats. Because LFB staining reflects the density and integrity of myelinated fibers, it is widely used as an indirect histological indicator of myelination and is often interpreted to reflect oligodendrocyte maturation and remyelination.[43,44] The restoration of LFB intensity observed after ERCM administration therefore suggests the recovery of mature oligodendrocytes and active remyelination. Consistently, in parallel experiments with F3 and F3.Olig2 cells, ERCM protected against cell death by exerting anti-inflammatory effects and promoted cell proliferation, maturation, and differentiation into oligodendrocytes. These protective and therapeutic effects are likely attributable to the diverse functional molecules, including GFs, NFs, miRNAs, cytokines, and other proteins.[34] In particular, neurotrophins such as NT3, BDNF, and NGF, as detected in ERCM, have been shown to promote NSC and oligodendrocyte proliferation as well as differentiation into neurons and oligodendrocytes.[45] Similarly, CNTF enhances OPC proliferation and increases the rate of oligodendrocyte generation,[46,47] while GDNF stimulates OPC proliferation and differentiation into myelinating oligodendrocytes.[48] In agreement with these findings, our double immunostaining revealed that ERCM significantly increased PDGFR-positive cells and enhanced Sox10/Olig2 co-localization in the corpus callosum, further confirming that ERCM facilitates oligodendrocyte differentiation and maturation through PDGF-mediated signaling.[40–42]

Taken together, our findings demonstrate that ERCM exerts robust neuroprotective and regenerative effects in vitro and in vivo through anti-inflammatory, pro-survival, and oligodendrogenic mechanisms. Although the lack of long-term behavioral testing remains a limitation, the present results indicate that ERCM represents a promising candidate for the treatment of CP. Future studies incorporating extended behavioral assessments and comprehensive proteomic profiling will be essential to further validate and expand upon these findings.

Conclusions

Developing therapeutic agents for neurological diseases is challenging because of the fact that they should fulfill the requirements necessary to prevent cell death by causative substance removal, damaged host cell proliferation, and neurobehavioral dysfunction improvement. However, in this study, ERCM exerted protective activity against LPS- or KCN-damaged F3 and F3.Olig2 cells and improved physical and cognitive HIL-induced abnormalities at PND5, which may be associated with enhanced expression of oligodendrocyte lineage markers and neuroprotective effects in vivo. Therefore, ERCM may present a promising candidate for treating CP.

Acknowledgments

Not applicable.

Author contributions

Eun-Jung Yoon (Formal analysis [equal], Investigation [equal], Methodology [equal], Visualization [equal], Writing—original draft [equal]), Jiwon Jeong (Data curation [equal], Formal analysis [equal], Investigation [equal], Methodology [equal], Visualization [equal], Writing—original draft [equal]), Yunseo Choi (Formal analysis [equal], Investigation [equal]), Dae Hwan Kim (Data curation [equal], Formal analysis [equal]), Tae Myoung Kim (Supervision [equal], Validation [equal]), Ehn-Kyoung Choi (Supervision [equal], Validation [equal]), Yun-Bae Kim (Conceptualization [equal], Project administration [equal], Writing—review & editing [equal]), and Dongsun Park (Conceptualization [equal], Project administration [equal], Visualization [equal], Writing—review & editing [equal])

Supplementary material

Supplementary material is available at *Stem Cells Translational Medicine* online.

Funding

This research was supported by the Basic Science Research Program of the National Research Foundation of Korea (NRF), funded by the Ministry of Education (NRF-2022R1A2C1003624).

Conflicts of interest

None declared.

Data availability

The datasets used and/or analyzed during the current study are available from the corresponding author on reasonable request.

Ethics approval

All animal experiments were performed following the standard operating procedures of the Laboratory Animal Center, Chungbuk National University (CBNU), Korea. The study protocol was approved by the Institutional Animal Care and Use Committee of the CBNU (#CBNUA-1720-22-02).

References

1. Hagberg H, Peebles D, Mallard C. Models of white matter injury: comparison of infectious, hypoxic-ischemic, and excitotoxic insults. *Ment Retard Dev Disabil Res Rev*. 2002;8:30-38. https://doi.org/10.1002/mrdd.10007
2. Kim TK, Park D, Ban YH, et al. Improvement by human oligodendrocyte progenitor cells of neurobehavioral disorders in an experimental model of neonatal periventricular leukomalacia. *Cell Transplant*. 2018;27:1168-1177. https://doi.org/10.1177/0963689718781330

3. Volpe JJ. Brain injury in premature infants: a complex amalgam of destructive and developmental disturbances. *Lancet Neurol*. 2009;8:110-124. https://doi.org/10.1016/S1474-4422(08)70294-1
4. Deng W, Pleasure J, Pleasure D. Progress in periventricular leukomalacia. *Arch Neurol*. 2008;65:1291-1295. https://doi.org/10.1001/archneur.65.10.1291
5. Wilson-Costello D, Friedman H, Minich N, Fanaroff AA, Hack M. Improved survival rates with increased neurodevelopmental disability for extremely low birth weight infants in the 1990s. *Pediatrics*. 2005;115:997-1003. https://doi.org/10.1542/peds.2004-0221
6. Back SA, Han BH, Luo NL, et al. Selective vulnerability of late oligodendrocyte progenitors to hypoxia-ischemia. *J Neurosci*. 2002;22:455-463. https://doi.org/10.1523/JNEUROSCI.22-02-00455.2002
7. Rivkin MJ, Volpe JJ. Hypoxic-ischemic brain injury in the newborn. *Semin Neurol*. 1993;13:30-39. https://doi.org/10.1055/s-2008-1041104
8. Back SA, Riddle A, McClure MM. Maturation-dependent vulnerability of perinatal white matter in premature birth. *Stroke*. 2007;38:724-730. https://doi.org/10.1161/01.STR.0000254729.27386.05
9. Back SA, Luo NL, Borenstein NS, Levine JM, Volpe JJ, Kinney HC. Late oligodendrocyte progenitors coincide with the developmental window of vulnerability for human perinatal white matter injury. *J Neurosci*. 2001;21:1302-1312. https://doi.org/10.1523/JNEUROSCI.21-04-01302.2001
10. Kinney HC, Back SA. Human oligodendroglial development: relationship to periventricular leukomalacia. *Semin Pediatr Neurol*. 1998;5:180-189. https://doi.org/10.1016/s1071-9091(98)80033-8
11. Oka A, Belliveau MJ, Rosenberg PA, Volpe JJ. Vulnerability of oligodendroglia to glutamate: pharmacology, mechanisms, and prevention. *J Neurosci*. 1993;13:1441-1453. https://doi.org/10.1523/JNEUROSCI.13-04-01441.1993
12. Azzopardi DV, Strohm B, Edwards AD, et al.; TOBY Study Group. Moderate hypothermia to treat perinatal asphyxial encephalopathy. *N Engl J Med*. 2009;361:1349-1358. https://doi.org/10.1056/NEJMoa0900854
13. Rees S, Harding R, Walker D. The biological basis of injury and neuroprotection in the fetal and neonatal brain. *Int J Dev Neurosci*. 2011;29:551-563. https://doi.org/10.1016/j.ijdevneu.2011.04.004
14. Park D, Shin K, Choi EK, et al. Protective effects of N-acetyl-L-cysteine in human oligodendrocyte progenitor cells and restoration of motor function in neonatal rats with hypoxic-ischemic encephalopathy. *Evid Based Complement Alternat Med*. 2015;2015:764251. https://doi.org/10.1155/2015/764251
15. Aly H, Abd-Rabboh L, El-Dib M, et al. Ascorbic acid combined with ibuprofen in hypoxic ischemic encephalopathy: a randomized controlled trial. *J Perinatol*. 2009;29:438-443. https://doi.org/10.1038/jp.2009.1
16. Tsuji M, Wilson MA, Lange MS, Johnston MV. Minocycline worsens hypoxic-ischemic brain injury in a neonatal mouse model. *Exp Neurol*. 2004;189:58-65. https://doi.org/10.1016/j.expneurol.2004.01.011
17. van der Kooij MA, Groenendaal F, Kavelaars A, Heijnen CJ, van Bel F. Combination of deferoxamine and erythropoietin: therapy for hypoxia-ischemia-induced brain injury in the neonatal rat? *Neurosci Lett*. 2009;451:109-113. https://doi.org/10.1016/j.neulet.2008.12.013
18. Kim SU, de Vellis J. Stem cell-based cell therapy in neurological diseases: a review. *J Neurosci Res*. 2009;87:2183-2200. https://doi.org/10.1002/jnr.22054
19. Hwang DH, Kim BG, Kim EJ, et al. Transplantation of human neural stem cells transduced with Olig2 transcription factor improves locomotor recovery and enhances myelination in the white matter of rat spinal cord following contusive injury. *BMC Neurosci*. 2009;10:117. https://doi.org/10.1186/1471-2202-10-117
20. Park D, Lee SH, Bae DK, et al. Transplantation of human adipose tissue-derived mesenchymal stem cells restores the neurobehavioral disorders of rats with neonatal hypoxic-ischemic encephalopathy. *Cell Med*. 2013;5:17-28. https://doi.org/10.3727/215517913x658936
21. Raposo G, Stoorvogel W. Extracellular vesicles: exosomes, microvesicles, and friends. *J Cell Biol*. 2013;200:373-383. https://doi.org/10.1083/jcb.201211138
22. Patil M, Henderson J, Luong H, Annamalai D, Sreejit G, Krishnamurthy P. The art of intercellular wireless communications: exosomes in heart disease and therapy. *Front Cell Dev Biol*. 2019;7:315. https://doi.org/10.3389/fcell.2019.00315
23. Cui GH, Wu J, Mou FF, et al. Exosomes derived from hypoxia-preconditioned mesenchymal stromal cells ameliorate cognitive decline by rescuing synaptic dysfunction and regulating inflammatory responses in APP/PS1 mice. *Faseb J*. 2018;32:654-668. https://doi.org/10.1096/fj.201700600R
24. Yoon EJ, Choi Y, Kim TM, Choi EK, Kim YB, Park D. The neuroprotective effects of exosomes derived from TSG101-overexpressing human neural stem cells in a stroke model. *Int J Mol Sci*. 2022;23:9532. https://doi.org/10.3390/ijms23179532
25. Kang D, Kang MJ, Kong D, et al. Effect of human amniotic epithelial stem cell transplantation on preterm premature rupture of fetal membrane using the amniotic pore culture technique in vitro. *Gynecol Obstet Invest*. 2022;87:333-343. https://doi.org/10.1159/000527514
26. Park D, Lee HJ, Joo SS, et al. Human neural stem cells over-expressing choline acetyltransferase restore cognition in rat model of cognitive dysfunction. *Exp Neurol*. 2012;234:521-526. https://doi.org/10.1016/j.expneurol.2011.12.040
27. Yon J-M, Kim Y-B, Park D. The ethanol fraction of white rose petal extract abrogates excitotoxicity-induced neuronal damage in vivo and in vitro through inhibition of oxidative stress and proinflammation. *Nutrients*. 2018;10:1375. https://doi.org/10.3390/nu10101375
28. Seong HR, Noh CH, Park S, et al. Intraocular pressure-lowering and retina-protective effects of exosome-rich conditioned media from human amniotic membrane stem cells in a rat model of glaucoma. *Int J Mol Sci*. 2023;24:8073. https://doi.org/10.3390/ijms24098073
29. Banks WA, Sharma P, Bullock KM, Hansen KM, Ludwig N, Whiteside TL. Transport of extracellular vesicles across the blood-brain barrier: brain pharmacokinetics and effects of inflammation. *Int J Mol Sci*. 2020;21:4407. https://doi.org/10.3390/ijms21124407
30. Follett PL, Deng W, Dai W, et al. Glutamate receptor-mediated oligodendrocyte toxicity in periventricular leukomalacia: a protective role for topiramate. *J Neurosci*. 2004;24:4412-4420. https://doi.org/10.1523/JNEUROSCI.0477-04.2004
31. Choi E-K, Park D, Kim TK, et al. Animal models of periventricular leukomalacia. *Lab Anim Res*. 2011;27:77-84.
32. Park D, Kim TK, Choi YJ, et al. Experimental models of cerebral palsy in infant rats. *Lab Anim Res*. 2010;26:345-351.
33. Yoon EJ, Jeong J, Park Y, Park D. The effect on differentiation and maturation of oligodendrocyte by age of cerebral palsy modeling using Sprague Dawley rat. *Brain, Digital, & Learning*. 2023;13:309-321.
34. Gurunathan S, Kang MH, Kim JH. A comprehensive review on factors influences biogenesis, functions, therapeutic and clinical implications of exosomes. *Int J Nanomedicine*. 2021;16:1281-1312. https://doi.org/10.2147/IJN.S291956
35. Zhou Y, He LN, Wang LN, et al. Human amniotic mesenchymal stromal cell-derived exosomes promote neuronal function by inhibiting excessive apoptosis in a hypoxia/ischemia-induced cerebral palsy model: a preclinical study. *Biomed Pharmacother*. 2024;173:116321. https://doi.org/10.1016/j.biopha.2024.116321
36. Chen X, Sai Y, Cui W, et al. Human umbilical cord mesenchymal stem cell-derived exosomes combined with mouse nerve growth factor can more effectively ameliorate the motor disorder and brain pathological injury in mice with cerebral palsy. *Adv Clin Exp Med*. 2025;34:911-923. https://doi.org/10.17219/acem/192773

37. Isildar B, Ozkan S, Koyuturk M. Preconditioning of human umbilical cord mesenchymal stem cells with a histone deacetylase inhibitor: valproic acid. *Balkan Med J*. 2024;41:369-376. https://doi.org/10.4274/balkanmedj.galenos.2024.2024-6-25
38. Olcar HN, Isildar B, Ozkan S, Ercin M, Gezginci-Oktayoglu S, Koyuturk M. Investigation of conditioned medium properties obtained from human umbilical cord mesenchymal stem/stromal cells preconditioned with dimethyloxalylglycine in a correlation with ultrastructural changes. *Microsc Res Tech*. 2024;87:159-171. https://doi.org/10.1002/jemt.24420
39. Ohtake Y, Park D, Abdul-Muneer PM, et al. The effect of systemic PTEN antagonist peptides on axon growth and functional recovery after spinal cord injury. *Biomaterials*. 2014;35:4610-4626. https://doi.org/10.1016/j.biomaterials.2014.02.037
40. Calver AR, Hall AC, Yu WP, et al. Oligodendrocyte population dynamics and the role of PDGF in vivo. *Neuron*. 1998;20:869-882. https://doi.org/10.1016/s0896-6273(00)80469-9
41. Finzsch M, Stolt CC, Lommes P, Wegner M. Sox9 and Sox10 influence survival and migration of oligodendrocyte precursors in the spinal cord by regulating PDGF receptor alpha expression. *Development*. 2008;135:637-646. https://doi.org/10.1242/dev.010454
42. Sock E, Wegner M. Using the lineage determinants Olig2 and Sox10 to explore transcriptional regulation of oligodendrocyte development. *Dev Neurobiol*. 2021;81:892-901. https://doi.org/10.1002/dneu.22849
43. Atkinson S, Li YQ, Wong CS. Changes in oligodendrocytes and myelin gene expression after radiation in the rodent spinal cord. *Int J Radiat Oncol Biol Phys*. 2003;57:1093-1100. https://doi.org/10.1016/s0360-3016(03)00735-1
44. Tisoncik-Go J, Stokes C, Whitmore LS, et al. Disruption of myelin structure and oligodendrocyte maturation in a macaque model of congenital zika infection. *Nat Commun*. 2024;15:5173. https://doi.org/10.1038/s41467-024-49524-2
45. Langhnoja J, Buch L, Pillai P. Potential role of NGF, BDNF, and their receptors in oligodendrocytes differentiation from neural stem cell: an in vitro study. *Cell Biol Int*. 2021;45:432-446. https://doi.org/10.1002/cbin.11500
46. Barres BA, Burne JF, Holtmann B, Thoenen H, Sendtner M, Raff MC. Ciliary neurotrophic factor enhances the rate of oligodendrocyte generation. *Mol Cell Neurosci*. 1996;8:146-156. https://doi.org/10.1006/mcne.1996.0053
47. Talbott JF, Cao Q, Bertram J, et al. CNTF promotes the survival and differentiation of adult spinal cord-derived oligodendrocyte precursor cells in vitro but fails to promote remyelination in vivo. *Exp Neurol*. 2007;204:485-489. https://doi.org/10.1016/j.expneurol.2006.12.013
48. Vaes JEG, Brandt MJV, Wanders N, et al. The impact of trophic and immunomodulatory factors on oligodendrocyte maturation: potential treatments for encephalopathy of prematurity. *Glia*. 2021;69:1311-1340. https://doi.org/10.1002/glia.23939